Inorg. Chem. **2009**, *48*, 4277−4289

Solvation of $Ln^{(III)}$ Lanthanide Cations in the [BMI][SCN], [$MeBu_3N$][SCN], and $[BMI]_5[Ln(NCS)_8]$ Ionic Liquids: A Molecular Dynamics Study

A. Chaumont and G. Wipff*

Institut de Chimie, Université Louis Pasteur, 4 rue B. Pascal, Strasbourg 67 000, France

Received November 20, 2008

We report a molecular dynamics study on the solvation of trivalent lanthanide cations $Ln^{(III)}$ (Ln = La, Eu and Yb) in the [BMI][SCN] and [$MeBu_3N$][SCN] ionic liquids (ILs), based respectively on 1-methyl-3-butylimidazolium (BMI^+) and tributylmethylammonium ($MeBu_3N^+$) cations, and on thiocyanate (SCN^-) anions. For this purpose we first derive a force field representation of SCN^- that simultaneously describes the [BMI][SCN] liquid and SCN^- as a ligand for $Ln^{(III)}$ ions and, in particular, for the energy difference between N- vs S-coordination, as compared to QM calculated values. In liquid simulations, we compare different initial states where the solute is either the "naked" $Ln^{(III)}$ ion or its anionic $Ln(NCS)_8^{5-}$ complex. In all cases, the first solvation shell of $Ln^{(III)}$ is found to be purely anionic, with 6 to 8 N-coordinated ligands, depending on the nature of $Ln^{(III)}$ and the immersed solute. This first shell is surrounded by 13 − 14 BMI^+ or 8 − 9 $MeBu_3N^+$ cations, leading to an "onion type" solvation of $Ln^{(III)}$. The comparison of gas phase optimized structures (that are all unstable from $n = 5$ NCS^- ligands) to those observed in ILs points to the importance of solvation forces on the nature of the $Ln^{(III)}$ complex, with a marked contribution of the IL cation. A given $Ln(NCS)_n^{3-n}$ complex is found to be better stabilized by the imidazolium than by the ammonium based IL. Furthermore, according to free energy PMF (potential of mean force) calculations, the imidazolium based liquid favors somewhat higher coordination numbers (CNs), compared to the ammonium based IL. For instance, the coordination of an eight SCN^- ligand to $Eu(NCS)_7^{4-}$ is favored in the [BMI][SCN] liquid, but not in [$MeBu_3N$][SCN]. For the $La^{(III)}$ and $Yb^{(III)}$ cations, the CNs are the same in both liquids (8 and 7, respectively), but the free energy differences between the two types of complexes differ markedly. The final part of the paper is devoted to the $[BMI]_5[Ln(NCS)_8]$ pure ILs, based on BMI^+ as cation and on the $Ln(NCS)_8^{5-}$ complex (Ln = $La^{(III)}$ and $Yb^{(III)}$) as anionic component. In these liquids, $Ln^{(III)}$ CNs are found to be similar to those found in the [BMI][SCN] solutions, and the dynamics is characterized by a fluid behavior of the BMI^+ ions diffusing around a quasi frozen network of anionic complexes.

Introduction

Salts with a temperature of fusion below 100 °C are commonly known as room temperature ionic liquids, or ionic liquids (ILs).[1−4] Their increasing popularity certainly comes from their non-measurable vapor pressure making them a potential "green" alternative to the commonly used volatile organic solvents.[5,6] ILs moreover possess many interesting properties like a wide liquidus range, good thermal stability, considerable electric conductivities, wide electrochemical windows making them interesting new solvents and materials for a large number of applications in various fields of chemistry such as electrochemistry, organic synthesis, and catalysis.[2,4] Another interesting feature is the fact that their physical properties can be fine-tuned by an adequate choice of their constitutive anions and cations. Commonly used ILs are based on imidazolium or ammonium cations and various inorganic anions such as PF_6^-, Tf_2N^-, NO_3^-, or BF_4^-. After the pioneering studies of chloroaluminate based ILs,[7] a new class of ILs has emerged, based on imidazolium cations and anionic metal complexes.[8−14] These liquids combine common physical properties of ILs and magnetic, photophysical/optical, and catalytic metal properties, opening the door for a new class of materials. Among them, ILs based on lanthanide cation complexes seem to be of great interest as they lead to not only luminescent but also magnetic properties that strongly depend on the coordination sphere of the lanthanide cation.[15] Recently, Nockemann et al. reported the

* To whom correspondence should be addressed. E-mail: wipff@chimie.u-strasbg.fr.

(1) Welton, T. *Chem. Rev.* **1999**, *99*, 2071–2083.
(2) Wasserscheid, P.; Welton, T. *Ionic Liquids in Synthesis*; Wiley-VCH: Weinheim, 2002; Vol. ISBN 3-527-30515-7.
(3) Wasserscheid, P.; Welton, T. *Ionic Liquids in Synthesis*, 2nd. ed (completely revised and enlarged version); Wiley-VCH: Weinheim, 2007.
(4) Visser, A. E.; Rogers, R. D. *J. Solid State Chem.* **2003**, *171*, 109–113.
(5) Rogers, R. D.; Seddon, K. R. *Science* **2003**, *302*, 792–793.
(6) Seddon, K. R. *J. Chem. Tech. Biotechnol.* **1997**, *68*, 351–356.
(7) Hussey, C. L. *Pure Appl. Chem.* **1988**, *60*, 1763.
(8) Sitze, M. S.; Schreiter, E. R.; Patterson, E. V.; Freeman, R. G. *Inorg. Chem.* **2001**, *40*, 2298–2304.
(9) Dullius, J. E. L.; Suarez, P. A. Z.; Einloft, S.; de Souza, R. F.; Dupont, J.; Fischer, J.; de Cian, A. *Organometallics* **1998**, 815–819.
(10) Del Sesto, R. E.; McCleskey, T. M.; Burrell, A. K.; Baker, G. A.; Thompson, J. D.; Scott, B. L.; Wilkes, J. S.; Williams, P. *Chem. Commun.* **2008**, 447–449.
(11) Mallick, B.; Balke, B.; Felser, C.; Mudring, A.-V. *Ang. Chem., Int. Ed.* **2008**, 7635–7638.
(12) Tang, S.; Babai, A.; Mudring, A.-V. *Ang. Chem., Int. Ed.* **2008**, 7631–7634.
(13) Yoshida, Y.; Saito, G. *J. Mater. Chem.* **2006**, *16*, 1254.
(14) Hayashi, S.; Hamaguchi, H. *Chem. Lett.* **2004**, *33*, 1590.

10.1021/ic802227p CCC: $40.75
Published on Web 02/09/2009

synthesis of anionic rare-earth thiocyanate complexes as building blocks of ILs, of general $[BMI]_{x-3}[Ln(NCS)_x(H_2O)_y]$ formula, where Ln = La−Yb, $x = 6-8$, $y = 0-2$, and BMI^+ stands for the 1-butyl-3-methylimidazolium cation.[16] In the X-ray structure of the $[BMI]_4[La(NCS)_7(H_2O)]$ compound, $La^{(III)}$ is coordinated to 7 SCN^- ligands and to an H_2O molecule, and its absorption characteristics are very similar to those of the corresponding liquid.[16] Likewise, dysprosium-based cyano complexes with imidazolium counterions form ILs combining strong luminescence and magnetic properties that markedly depend on the coordination sphere of the lanthanide cation.[11] An accurate knowledge of the solvation of lanthanides in ILs is therefore of utmost importance to develop such new materials. In synergy with experimental spectroscopic and diffraction approaches, when available, molecular dynamics (MD) simulations based on all-atom representation of the solution represent a powerful tool for studying the structure of ILs and their solvation properties toward all kinds of solutes. For a recent survey of simulations of ILs, see, for example, refs 17, 18 and, for the solvation of alkali, alkaline earth, lanthanide, and actinide cations by ILs, see refs 19−29. These methods have inherent limitations about the size of the systems (a few nanometers), the empirical representation of their energy (computerized ball-and-stick model, assuming that non-covalent interactions are mainly steric and Coulombic in nature), relatively short simulated times (nanoseconds), but offer the advantage of showing the time evolution of selected hypothetical structures, allowing us to analyze the different solvation shells of metallic centers. They also give insights into key interaction energy components of the system.

As a first step toward simulation of anionic lanthanide complexes-based ILs, we decided to first simulate by MD the solvation structure of three different trivalent lanthanides cations in the [BMI][SCN] and $[MeBu_3N][SCN]$ ILs based on the SCN^- anion and, respectively, on the BMI^+ and $MeBu_3N^+$ cations. We want mainly to investigate the nature of the first coordination shells in solution (and, as a reference, in the gas phase) comparing a big ($La^{(III)}$) to a small ($Yb^{(III)}$) and an intermediate sized ($Eu^{(III)}$) lanthanide cation. As a prerequisite, we briefly describe the pure [BMI][SCN] and $[MeBu_3N][SCN]$ ILs for which we had to develop force field parameters that also account for the coordination properties of SCN^- to $Ln^{(III)}$ ions. In crystal structures, the potentially ambidendate SCN^- ligand is N-coordinated, forming the hexacoordinated $Ln(NCS)_6^{3-}$ complexes,[30] as well as $Ln(NCS)_n^{3-n}$ complexes with $n = 7$ or 8 for $La^{(III)}$, 8 for $Eu^{(III)}$, 6 and 7 for $Yb^{(III)}$ (see Supporting Information, Table S1). It is thus important to determine what the different coordination numbers (CNs) in solution are, comparing imidazolium to ammonium containing liquids, and to describe the solvation features of the complexes. We next report free energy profiles (potential of mean force calculations) in the two liquids to compare the relative stabilities of 7- versus 8-coordinated $La^{(III)}$, $Eu^{(III)}$, and $Yb^{(III)}$ complexes and 6- to 7-coordinated $Yb^{(III)}$ complexes. The last part of the paper deals with the $[BMI]_5[Ln(NCS)_8]$ liquid, with $Ln(NCS)_8^{5-}$ complexes (Ln = La and Yb) as anionic component and BMI^+ cations as cationic component, with the main aims to test the stability of the octa-coordinated complexes with the two $Ln^{(III)}$ ions and to describe their solvation and dynamic properties.

Methods

Molecular Dynamics. The different systems were simulated by classical MD using the AMBER 7.0 software[31] in which the potential energy U is described by a sum of bond, angle, and dihedral deformation energies and pairwise additive 1-6-12 (electrostatic and van der Waals) interactions between non-bonded atoms:

$$U = \sum_{\text{bonds}} k_b(r - r_0)^2 + \sum_{\text{angles}} k_\theta(\theta - \theta_0)^2 + \sum_{\text{dihedrals}} \sum_n V_n(1 + \cos(n\varphi - \gamma)) + \sum_{i<j} \left[\frac{q_i q_j}{R_{ij}} - 2\varepsilon_{ij}\left(\frac{R^*_{ij}}{R_{ij}}\right)^6 + \varepsilon_{ij}\left(\frac{R^*_{ij}}{R_{ij}}\right)^{12} \right] \quad (1)$$

Cross terms in van der Waals interactions were constructed using the Lorentz−Berthelot rules. Force field parameters for BMI^+ cations were taken from the work of Andrade et al.,[32] while those for SCN^- anions had to be developed and will be discussed in the Results Section. The $MeBu_3N^+$ parameters were those used to study the $[MeBu_3N][Tf_2N]$ IL.[33] The $Ln^{(III)}$ parameters were fitted on free energies of hydration.[34]

1-4 van der Waals interactions were scaled down by 2.0 and 1-4 Coulombic interactions were scaled down by 1.2, as recommended by Cornell et al. [35] Pure liquids and solutions were simulated with 3D-periodic boundary conditions. Non-bonded interactions were calculated using a 12 Å atom based cutoff, correcting the long-range electrostatics by using the Ewald summation method in the Particle mesh Ewald (PME) approximation.

MD simulations were performed at constant temperature, starting with random velocities, using the Verlet leapfrog algorithm with a

(15) Binnemans, K. *Chem. Rev.* **2007**, *107*, 2592–2614, and references cited therein.
(16) Nockemann, P.; Thijs, B.; Postelmans, N.; van Hecke, K.; van Meervelt, L.; Binnemans, K. *J. Am. Chem. Soc.* **2006**, *128*, 13658–13659.
(17) Lynden-Bell, R. M.; Del Pópolo, M. G.; Youngs, T. G. A.; Kohanoff, J.; Hanke, C. G.; Harper, J. B.; Pinilla, C. C. *Acc. Chem. Res.* **2007**, *40*, 1138.
(18) Hunt, P. A.; Maginn, E. J.; Lynden-Bell, R. M.; Del Popolo, M. G. In *Ionic Liquids in Synthesis*, 2nd. ed (completely revised and enlarged version); Wasserscheid, P., Welton, T., Eds.; Wiley-VCH: Weinheim, 2007; Vol. *1*, pp 206−249.
(19) Vayssière, P.; Chaumont, A.; Wipff, G. *Phys. Chem. Chem. Phys.* **2004**, *7*, 124–135.
(20) Sieffert, N.; Wipff, G. *Phys. Chem. A* **2005**, *109*, 1106–1117.
(21) Chaumont, A.; Engler, E.; Wipff, G. *Inorg. Chem.* **2003**, *42*, 5348–5356.
(22) Chaumont, A.; Wipff, G. *Chem.—Eur. J.* **2004**, *10*, 3919–3930.
(23) Chaumont, A.; Wipff, G. *Inorg. Chem.* **2004**, *43*, 5891–5901.
(24) Chaumont, A.; Wipff, G. *Phys. Chem. Chem. Phys.* **2006**, *8*, 494–502.
(25) Chaumont, A.; Wipff, G. *Phys. Chem. Chem. Phys.* **2003**, *5*, 3481–3488.
(26) Chaumont, A.; Wipff, G. *J. Phys. Chem B* **2004**, *108*, 3311–3319.
(27) Chaumont, A.; Wipff, G. *Phys. Chem. Chem. Phys.* **2005**, *7*, 1926–1932.
(28) Gaillard, C.; Billard, I.; Chaumont, A.; Mekki, S.; Ouadi, A.; Denecke, M.; Moutiers, G.; Wipff, G. *Inorg. Chem.* **2005**, *44*, 8355–8367.
(29) Gaillard, C.; Chaumont, A.; Billard, I.; Hennig, C.; Ouadi, A.; Wipff, G. *Inorg. Chem.* **2007**, *46*, 4815–4826.
(30) Wickleder, M. S. *Chem. Rev.* **2002**, *102*, 2011–2088.
(31) Case, D. A.; Pearlman, D. A.; Caldwell, J. W.; Cheatham, T. E., III; Wang, J.; Ross, W. S.; Simmerling, C. L.; Darden, T. A.; Merz, K. M.; Stanton, R. V.; Cheng, A. L.; Vincent, J. J.; Crowley, M.; Tsui, V.; Gohlke, H.; Radmer, R. J.; Duan, Y.; Pitera, J.; Massova, I.; Seibel, G. L.; Singh, U. C.; Weiner, P. K.; Kollman, P. A. *AMBER7*; University of California: San Francisco, 2002.
(32) de Andrade, J.; Böes, E. S.; Stassen, H. *J. Phys. Chem. B* **2002**, *106*, 3546–3548.
(33) Schurhammer, R.; Wipff, G. *J. Phys. Chem. B* **2007**, *110*, 4659–4668.
(34) van Veggel, F. C. J. M.; Reinhoudt, D. *Chem.—Eur. J.* **1999**, *5*, 90–95.
(35) Cornell, W. D.; Cieplak, P.; Bayly, C. I.; Gould, I. R.; Merz, K. M.; Ferguson, D. M.; Spellmeyer, D. C.; Fox, T.; Caldwell, J. W.; Kollman, P. A. *J. Am. Chem. Soc.* **1995**, *117*, 5179–5197.

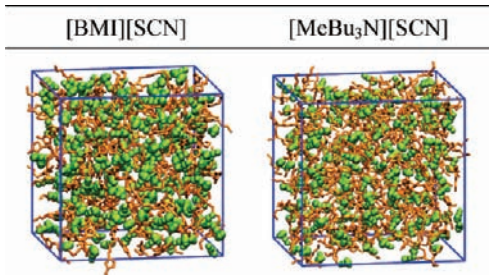

Figure 1. Typical simulation box of the [BMI][SCN] and [$MeBu_3N$][SCN] pure liquids (anions in green and cations in orange).

time step of 2 fs to integrate the equations of motion. The temperature was monitored by coupling the system to a thermal bath using the Berendsen algorithm with a relaxation time of 0.2 ps. All C−H bonds were constrained using the SHAKE algorithm.

We first equilibrated "cubic" boxes of pure liquids of about 40 Å length, containing about 200 BMI^+ or $MeBu_3N^+$ and SCN^- ions (see Figure 1). After equilibration the density of [BMI][SCN] (1.06 kg L^{-1}) was in good agreement with experimental data (1.07 kg L^{-1})[36] while that of [$MeBu_3N$][SCN] was smaller, 0.94 kg L^{-1}. To our knowledge, no experimental value has been reported for this liquid.

We then immersed the "naked" $Ln^{(III)}$ cation or its $Ln(NCS)_8^{5-}$ complex in the box, removing three solvent cations or five SCN^- anions to keep the box neutral. Equilibration started with 2000 steps of steepest descent energy minimization, followed by 100 ps with fixed solutes ("BELLY" option in AMBER) at constant volume, and by 250 ps of constant volume without constraints, followed by 500 ps at a constant pressure of 1 atm coupling the system to a barostat with a relaxation time of 0.2 ps. MD was then run for 5 ns in the (NVT) ensemble at 300 K for the [BMI][SCN] IL and 400 K for the [$MeBu_3N$][SCN] IL. We chose to simulate the [$MeBu_3N$][SCN] liquid at a higher temperature because ammonium based ILs are generally more viscous and have a higher fusion temperature than imidazolium based ILs (for example [NBu_4][Tf_2N] melts at 79 °C while [BMI][Tf_2N] melts at −3 °C).[37,38]

Simulation of $[BMI]_5[Ln(NCS)_8]$ pure ILs (Ln = La and Yb) started from a 3 × 3 × 3 grid of model built $Ln(NCS)_8^{5-}$ complexes around which we randomly placed 135 BMI^+ cations. The box was then equilibrated by repeated sequences of (i) heating the system at 500 K at constant volume for 0.4 ns, followed by (ii) 0.2 ns of dynamics at 300 K and a constant volume, and (iii) 1 ns of dynamics at 300 K and constant pressure of 1 atm. During the equilibration step the $Ln(NCS)_8^{5-}$ complexes were frozen using the BELLY option. The densities obtained after equilibration were 1.22 kg L^{-1} for the $[BMI]_5[La(NCS)_8]$ liquid (which is about 10% smaller than the experimental value of 1.35 kg L^{-1}),[16] and 1.19 kg L^{-1} for the $[BMI]_5[Yb(NCS)_8]$ liquid.

MD trajectories were saved every 1 ps and analyzed with the MDS and DRAW software.[39] Typical snapshots were redrawn using the VMD software.[40] The average solvent structure around $Ln^{(III)}$ was characterized by anion and cation radial distribution functions (RDFs) during the last 0.2 ns. Average CNs of solvent anions (N and S atoms of SCN^-) and cations (N_{butyl} atom of BMI^+, noted $N2_{BMI}$, or N_{MeBu3N} atom of $MeBu_3N^+$) were calculated up to the first peak minimum for the anions, and up to 10 Å for the cations for which the first peak was less well-defined. Insights into energy features were obtained by group component analysis, using a 12 Å cutoff distance and a PME correction for long-range electrostatics. In particular, the total potential energy of the system was decomposed as $U_{tot} = E_{complex} + E_{complex/IL} + E_{ILIL}$ where $E_{complex}$ is the internal energy of the $Ln(NCS)_n^{3-n}$ complex in solution, $E_{complex/IL}$ is the complex/solvent interaction energy ("solvation energy"), and E_{ILIL} corresponds to the intra solvent energy. The diffusion coefficients D were calculated from the Einstein equation: $6Dt = \langle[r_i(t) - r_i(0)]^2\rangle$ (where r_i is the position of atom i) and averaged over all identical species over the last nanoseconds of the dynamics.

Potential of Mean Force (PMF) Calculations on the Complexation of One NCS^- Anion by $Ln(NCS)_n^{3-n}$ Complexes. We calculated the free energy profiles for NCS^- complexation to $Ln(NCS)_7^{4-}$ complexes (Ln = La, Eu and Yb) in both [BMI][SCN] and [$MeBu_3N$][SCN] liquids. In the latter liquid, we similarly simulated the NCS^- uptake by $Yb(NCS)_6^{3-}$. Free energy profiles were calculated as a function of the $Ln-N_{NCS}$ distance (d) between the $Ln^{(III)}$ cation and the nearest non-coordinated NCS^- anion. The initial Ln−N distance d (ca. 8.5 Å for the different lanthanide cations) was obtained at the end of the MD runs and was stepwise decreased to 2.6 Å in the case of $La^{(III)}$, 2.4 Å in the case of $Eu^{(III)}$, and 2.3 Å in the case of $Yb^{(III)}$ (i.e., to average distances found in $Ln(NCS)_7^{4-}$ complexes). Transformation from the uncomplexed state to the complexed state was achieved in 51 steps, that is, with increments $\Delta\lambda$ of 0.02, corresponding to $\Delta d \sim 0.12$ Å. For each reaction three different equilibration and sampling times were tested (50 + 50 ps, 20 + 80 ps, and 25 + 100 ps at each step). Changes in free energy were calculated using the thermodynamic integration (TI) method based on eq 2.[41]

$$\Delta G = \int_0^1 \left\langle \frac{\partial U}{\partial \lambda} \right\rangle_\lambda \mathrm{d}\lambda \qquad (2)$$

Quantum Mechanics Calculations. Structures of the $Ln(NCS)_n^{3-n}$ and $Ln(SCN)_n^{3-n}$ complexes were optimized without symmetry constraints using the Gaussian03 software[42] at the HF and DFT levels of theory with the 6-31+G* basis set for the ligands. As f-orbitals do not play a major role in metal−ligand bonds,[43] the 46 core and 4f electrons of lanthanides were described by quasi-relativistic effective core potentials (ECP) of the Stuttgart group.[44,45] For the valence orbitals the affiliated (7s6p5d)/[5s4p3d] basis set was used, enhanced by an additional single f-function from ref 46.

(36) From the BASF web site (www.basionics.com) with the CAS number 344790-87-0 for the [BMI][SCN] liquid.
(37) Tokuda, H.; Hayamizu, K.; Ishii, K.; Susan, M. A. B. H.; Watanabe, M. *J. Phys. Chem. B* **2005**, *109*, 6103–6110.
(38) Ngo, H. L.; LeCompte, K.; Hargens, L.; McEwen, A. B. *Thermochim. Acta* **2000**, *357−358*, 97–102.
(39) Engler, E.; Wipff, G. In *Crystallography of Supramolecular Compounds*; Tsoucaris, G., Ed.; Kluwer: Dordrecht, 1996, pp 471−476.
(40) Humphrey, W.; Dalke, A.; Schulten, K. *J. Mol. Graphics* **1996**, *14*, 33–38.
(41) Kollman, P. *Chem. Rev.* **1993**, *93*, 2395–2417.
(42) Frisch, M. J.; Trucks, G. W.; Schlegel, H. B.; Scuseria, G. E.; Robb, M. A.; Cheesemann, J. R.; J. A. Montgomery, J.; Vreven, T.; Kudin, K. N.; Burant, J. C.; Millam, J. M.; Iyengar, S. S.; Tomasi, J.; Barone, V.; Mennucci, B.; Cossi, M.; Scalmani, G.; Rega, N.; Petersson, G. A.; Nakatsuji, H.; Hada, M.; Ehara, M.; Toyota, K.; Fukuda, R.; Hasegawa, J.; Ishida, M.; Nakajima, T.; Honda, Y.; Kitao, O.; Nakai, H.; Klene, M.; Li, X.; Knox, J. E.; Hratchian, H. P.; Cross, J. B.; Bakken, V.; Adamo, C.; Jaramillo, J.; Gomperts, R.; Stratmann, R. E.; Yazyev, O.; Austin, A. J.; Cammi, R.; Pornelli, C.; Ochterski, J. W.; Ayala, P. Y.; Morokuma, K.; Voth, G. A.; Salvador, P.; Dannenberg, J. J.; Zakrzewski, V. G.; Dapprich, S.; Daniels, A. D.; Strain, M. C.; Farkas, O.; Malick, D. K.; Rabuck, A. D.; Raghavachari, K.; Foresman, J. B.; Ortiz, J. V.; Cui, Q.; Baboul, A. G.; Clifford, S.; Cioslowski, J.; Stefanov, B. B.; Liu, G.; Liashenko, A.; Piskorz, P.; Komaromi, I.; Martin, R. L.; Fox, D. J.; Keith, T.; Al-Laham, M. A.; Peng, C. Y.; Nanayakarra, A.; Challacombe, M.; Gill, P. M. W.; Johnson, B.; Chen, W.; Wong, W.; Gonzalez, C.; Pople, J. A., *Gaussian 03*; Gaussian,Inc.: Wallingford, CT, 2004.
(43) Maron, L.; Eisenstein, O. *J. Phys. Chem. A* **2000**, *104*, 7140–7143.

Table 1. Energy Change (kcal/mol) upon Successive Addition of up to 5 NCS^- Anions to the $Ln(NCS)_3$ Complexes in the Gas Phase: Comparison of QM (HF and DFT) Results to AMBER (3-PT, 5-PT-I, and 5PT-II) Results

reaction	HF (6-31+G*)	DFT (B3LYP/6-31+G*)	AMBER (3-PT)	AMBER (5-PT-I)	AMBER (5-PT-II)
$La(NCS)_3 \rightarrow La(NCS)_4^-$	−82.3	−75.9	−112.1	−113.4	−108
$La(NCS)_4^- \rightarrow La(NCS)_5^{2-}$	−0.6	5.6	−41.4	−41.5	−39
$La(NCS)_5^{2-} \rightarrow La(NCS)_6^{3-}$	53.3	60.0	18.4	22.3	19
$La(NCS)_6^{3-} \rightarrow La(NCS)_7^{4-}$	118.9	123.7	94.0	100.9	95
$La(NCS)_7^{4-} \rightarrow La(NCS)_8^{5-}$	166.4	171.4	158.8	162.2	155
$Eu(NCS)_3 \rightarrow Eu(NCS)_4^-$	−85.3	−82.3		−120.3	−88.0
$Eu(NCS)_4^- \rightarrow Eu(NCS)_5^{2-}$	−0.1	6.2		−46.0	−45.2
$Eu(NCS)_5^{2-} \rightarrow Eu(NCS)_6^{3-}$	54.8	61.7		20.6	18.0
$Eu(NCS)_6^{3-} \rightarrow Eu(NCS)_7^{4-}$	124.6	129.0		108.6	101.8
$Eu(NCS)_7^{4-} \rightarrow Eu(NCS)_8^{5-}$	172.0	176.7		228.2	163.4
$Yb(NCS)_3 \rightarrow Yb(NCS)_4^-$	−63.3	−59.0		−134.6	−129.4
$Yb(NCS)_4^- \rightarrow Yb(NCS)_5^{2-}$	−23.9	−19.4		−49.5	−49.2
$Yb(NCS)_5^{2-} \rightarrow Yb(NCS)_6^{3-}$	56.5	63.3		19.8	16.8
$Yb(NCS)_6^{3-} \rightarrow Yb(NCS)_7^{4-}$	131.2	135.1		120.6	112.9
$Yb(NCS)_7^{4-} \rightarrow Yb(NCS)_8^{5-}$	177.7	182.2		184.4	174.3

Results

1. Force Field Parameters for SCN. As no force field was available for ILs based on SCN^-, we had to develop parameters for this anion. The challenge was to simultaneously describe in a satisfactory manner the [BMI][SCN] liquid and its solvation properties toward $Ln^{(III)}$ cations, and therefore SCN^- as a ligand coordinated to $Ln^{(III)}$. For this purpose, five criteria (i) to (v) were considered. To describe the pure [BMI][SCN] liquid, we wanted to account (i) for the interaction energy between its constitutive ions in the gas phase and (ii) for the density of the liquid. Furthermore, for the SCN^- binding to the $Ln^{(III)}$ ions, we considered in the gas phase: (iii) the energy and structure of N- versus S-coordinated ligands in $La(NCS)_6^{3-}$ and $La(SCN)_6^{3-}$ complexes, and (iv) the complexation energy of up to five SCN^- anions to the $La(NCS)_3$ complex. Finally, (v) a MD simulation of the $Ln^{(III)}$ ion in the [BMI][SCN] liquid was performed to test whether all SCN^- ligands are N-coordinated. Gas phase reference data were obtained by QM calculations at the HF and DFT levels of theory.

We thus successively developed three SCN^- models: a three point model "3-PT" with atomic charges derived from QM calculations, and two five point models "5-PT-I" and "5-PT-II" with explicit lone pairs "LP"s on sulfur. Their characteristics are gathered in Supporting Information, Table S2. In the 5-PT-I model, the LPs bear the q_S charge of the 3-PT model (with some minor adjustements), while their van der Waals parameters are taken from the AMBER force field.[35] The 5-PT-II parameters have been obtained by fine-tuning (by trial and errors) the 5-PT-I charges and van der Waals parameters to improve the structures and relative stabilities of $La(NCS)_6^{3-}$ and $La(SCN)_6^{3-}$ complexes in the gas phase, as compared to those obtained by QM methods.

The three models satisfy criteria (i) and (ii): the interaction energy between MMI^+ (MMI^+ is the 1,3-dimethylimidazolium cation, a simple model for BMI^+) and SCN^- are −81.3, −82.7, and −80.7 kcal/mol, respectively, that is, close to the QM calculated values (−79.6 kcal/mol at the HF level and −82.7 kcal/mol at the DFT level),[47] and the calculated densities of the [BMI][SCN] liquid (1.09, 1.11, and 1.06 kg L^{-1}, respectively) are close to the experimental value of 1.07 kg L^{-1}. [36] Criteria (iii) and (v) were neither satisfied with the 3-PT nor 5-PT-I models: the energy preference for N- over S-coordination in the hexa-coordinated $La^{(III)}$ complex was only 10 and 50 kcal/mol, respectively, which is too small, compared to the QM values (79.8 kcal/mol at the HF level and 81.5 kcal/mol by DFT; see Supporting Information, Table S3). Thus, when the "naked" $La^{(III)}$ ion was simulated in the [BMI][SCN] liquid, it coordinated 7 to 8 SCN^- anions with both models, but some of them were S-coordinated (five with the 3-PT model and four with the 5-PT-I model).

With the 5-PT-II model, agreement with reference values was more satisfactory. The energy preference for N- coordination in the $La^{(III)}$ hexa- complex was 78.0 kcal/mol and, in the [BMI][SCN] solution all SCN^- anions that spontaneously complexed to $La^{(III)}$ during the dynamics were N-coordinated. The same binding feature was observed for the $Eu^{(III)}$ and $Yb^{(III)}$ ions in the IL solutions (vide infra). Futhermore, the 5-PT-II parameters give satisfactory energy trends for the N- versus S-coordination in the gas phase for the other lanthanide complexes ($Eu(NCS)_6^{3-}$ versus $Eu(SCN)_6^{3-}$ and $Yb(NCS)_6^{3-}$ versus $Yb(SCN)_6^{3-}$; see Supporting Information, Table S3). They also account for the successive addition of up to five SCN^- anions to $Ln(NCS)_3$ complexes (see Table 1). In particular for the reactions:

(44) Dolg, M.; Stoll, H.; Savin, A.; Preuss, H. *Theoret. Chim. Acta* **1989**, *75*, 173–194.
(45) Dolg, M.; Stoll, H.; Savin, A.; Preuss, H. *Theoret. Chim. Acta* **1993**, *85*, 441–450.
(46) Ehlers, A. W.; Böhme, M.; Dapprich, S.; Gobbi, A.; Höllwarth, A.; Jonas, V.; Köhler, K. F.; Stegmann, R.; Veldkamp, A.; Frenking, G. *Chem. Phys. Lett.* **1993**, *208*, 111.

(47) Note that the structure of the MMI^+ SCN^- dimer optimized with AMBER somewhat differs from the QM optimized one. Compare for instance, the 5-PT-II, HF and DFT results: the $N_{SCN}-H2_{MMI}$ distance is 2.65 Å (AMBER), 2.31 Å (HF), 2.10 Å (DFT); the $S_{SCN}-H2_{MMI}$ distance is 3.25 Å (AMBER), 2.90 Å (HF), 2.92 Å (DFT). The longer distances obtained with AMBER correspond in fact to somewhat different arrangements: the SCN^- anion sits tangential to the imidazolium ring in the HF and DFT optimized structures, but somewhat above the imidazolium ring in the AMBER structure. The first geometry favors more linear H-bonds involving SCN^- $l\sigma^*_{C\text{-}H}$ orbital interactions, reminiscent of the Cl^- $l\sigma^*_{C\text{-}H}$ interactions found by CP-MD simulations in the [MMI][Cl] IL (see. Bühl, M.; Chaumont, A.; Schurhammer, R.; Wipff, G. *J. Phys. Chem. B* **2005**, *109*, 18591–18599; Clearly, this feature cannot be reproduced with a simple force field.

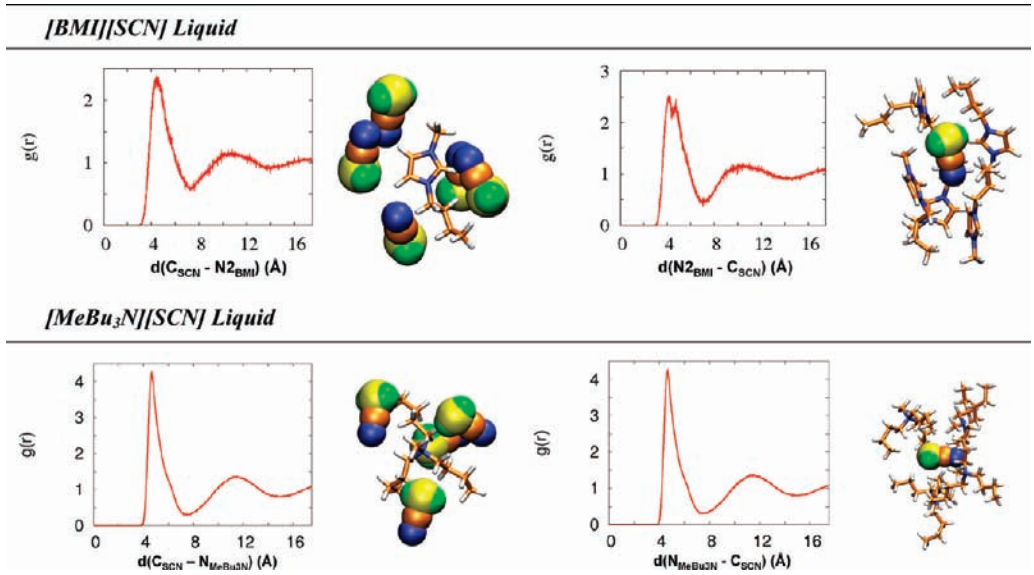

Figure 2. [BMI][SCN] and [$MeBu_3N$][SCN] pure liquids: Radial distribution functions and typical snapshots of the 1st solvation shell of BMI^+ and SCN^- ions (top row) or $MeBu_3N^+$ and SCN^- ions (bottom row).

$$Ln(NCS)_6^{3-} + SCN^- \rightarrow Ln(NCS)_7^{4-}$$

and

$$Ln(NCS)_7^{4-} + SCN^- \rightarrow Ln(NCS)_8^{5-}$$

that are crucial in solution, 5-PT-II energies are very close to QM ones. Note that, according to force field and QM results, coordination of additional SCN^- anions to the negatively charged $Ln(NCS)_5^{2-}$ complex is disfavored in the gas phase. Regarding the structures of these AMBER optimized complexes, one sees that the N-coordination is linear (Ln−N−S = 180°) while the less stable S-coordination is bent (Ln−S−N ≈ 115°), as found by QM calculations (see Supporting Information, Table S4). Thus, the 5-PT-II model that satisfactorily describes the [BMI][SCN] IL and the energy and stereochemical features of the lanthanide complexes in the gas phase and in the IL solutions was used throughout this study.

2. Pure [BMI][SCN] and [$MeBu_3N$][SCN] ILs. Typical snapshots of cations and anions surroundings in the [BMI]-[SCN] and [$MeBu_3N$][SCN] liquids as well as cation−anion RDFs ($N2_{BMI}\cdots C_{SCN}$ and $N_{MeBu3N}\cdots C_{SCN}$) are given in Figure 2.

In the [BMI][SCN] liquid, one finds on the average 5.4 BMI^+ cations within 7 Å of SCN^- anions and 5.8 SCN^- anions within 7.3 Å of BMI^+ cations. BMI^+ cations mainly interact via their C−H ring protons with the N_{SCN} or the LP_{SCN} sites of SCN^-, as seen from proton density maxima around the SCN^- anions (Figure 3). The SCN^- orientation around BMI^+ cations is mainly tangential, with N_{SCN} and S_{NCS} density peaks being at similar distances from the imidazolium ring (2.5 Å for N_{SCN} and 2.7 Å for S_{SCN}). In the [$MeBu_3N$][SCN] liquid one finds on the average 4.0 $MeBu_3N^+$ cations within 7.2 Å of a SCN^- anion and 4.3 SCN^- anions within 7.6 Å of a $MeBu_3N^+$ cation (Figure 2). In that liquid, there is no particular interaction pattern between anions and cations, as seen from the "spherical" distribution of proton density around SCN^- (Figure 3).

Calculated diffusion coefficients *D*, averaged over the last nanoseconds of dynamics (in 10^{-8} cm^2/s) are 8.5 for BMI^+ cations and 6.8 for SCN^- anions in [BMI][SCN], and 5.9 for $MeBu_3N^+$ and 4.9 for SCN^- in [$MeBu_3N$][SCN]. To our knowledge there are no experimental values available for these liquids, but we note that the calculated values are within those obtained for other imidazolium based ILs like [BMI]-[PF_6] (calculated values during 1 ns, in 10^{-8} cm^2/s: 7.9 for BMI^+ and 2.9 for PF_6^-; experimental values: 8.0 for BMI^+ and 5.8 for PF_6^-).[48] Furthermore they are consistent with the fact that ammonium based ILs are more viscous than imidazolium based ILs. Figure 4 displays cumulated positions of three BMI^+, $MeBu_3N^+$and SCN^- ions during the last 3 ns, showing that their motions mainly correspond to librations and rotations in a given potential well, instead of significant translations.

3. Solvation of $Ln^{(III)}$ Cations and of Their $Ln(NCS)_n^{3-n}$ Complexes in the [BMI][SCN] and [$MeBu_3N$][SCN] IL. In this section, we describe the solvation of $La^{(III)}$, $Eu^{(III)}$, and $Yb^{(III)}$ cations of decreasing size (and presumably decreasing CNs) in the [BMI][SCN] and [$MeBu_3N$][SCN] liquids. In principle, after equilibration of the system, the cation's CN should be independent of the starting state. ILs are however quite viscous, and their ion's diffusion is quite slow. According to experiments and simulations,[52−54] relaxation times are in the order of the multi-nanosecond time scale, which may raise sampling issues in the computations. This is why we considered for each lanthanide cation different

(48) Tokuda, H.; Hayamizu, K.; Ishii, K.; Susan, M. A. B. H.; Watanabe, M. *J. Phys. Chem. B* **2004**, *108*, 16593–16600.
(49) Aki, S. N. V. K.; Brennecke, J. F.; Samanta, A. *Chem. Commun.* **2001**, 413–414.
(50) Karmakar, R.; Samanta, A. *J. Phys. Chem. A* **2003**, *107*, 7340–7346.
(51) Grodkowski, J.; Neta, P.; Wishart, J. F. *J. Phys. Chem. A* **2003**, *107*, 9794–9799.
(52) Jeong, D.; Shim, Y.; Choi, M. Y.; Kim, H. J. *J. Phys. Chem. B* **2007**, *111*, 4920–4925.
(53) Znamenskiy, V.; Kobrak, M. N. *J. Phys. Chem. B* **2004**, *108*, 1072–1079.
(54) Kobrak, M. N.; Znamenskiy, V. *Chem. Phys. Lett.* **2004**, *395*, 127–132.

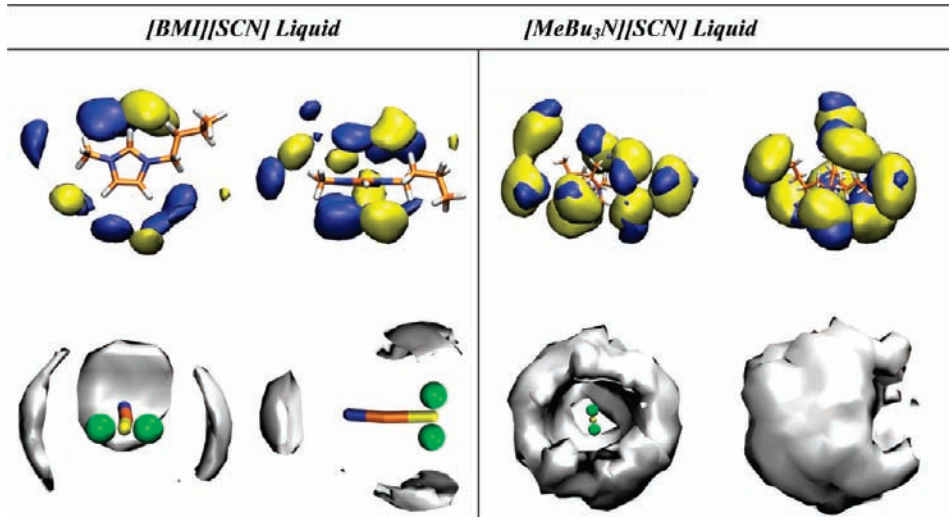

Figure 3. [BMI][SCN] and [$MeBu_3N$][SCN] pure liquids. First row: density maps of the N (blue) and S (yellow) atoms of SCN^- around the BMI^+ and $MeBu_3N^+$ cations. Second row: density maps of the BMI^+ imidazolium ring protons (left) and of the $MeBu_3N^+$ terminal protons around SCN^- (right).

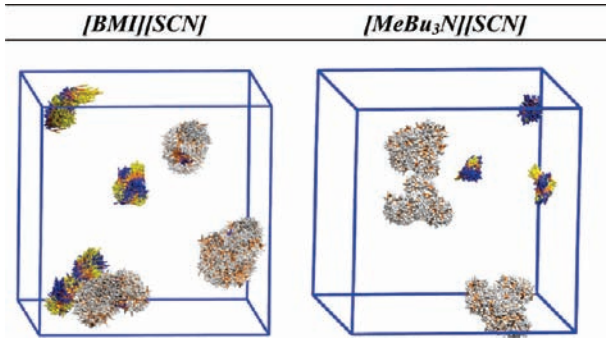

Figure 4. [BMI][SCN] and [$MeBu_3N$][SCN] pure liquids: Cumulative views over the last 3 ns of three randomly chosen BMI^+ or $MeBu_3N^+$ and SCN^- ions.

initial states, where it was immersed either as a "naked" $Ln^{(III)}$ species or as a preformed $Ln(NCS)_8^{5-}$ anionic complex. Characteristics of the simulated systems are given in Table 2. Typical snapshots and RDFs for the [BMI][SCN] and [$MeBu_3N$][SCN] solutions are shown in Figure 5, and the RDFs characteristics are summarized in Table 3, indicating the final CN of $Ln^{(III)}$.

Lanthanide Coordination Number. When $Ln(NCS)_8^{5-}$ complexes were immersed in the solution, the three simulated cations retained their 8-coordination in the two liquids. There was an exception in the case of $Yb(NCS)_8^{5-}$ that lost one SCN^- ligand in [$MeBu_3N$][SCN], but not in [BMI][SCN], hinting at an IL modulation of the CN (vide infra).

On the other hand, when "naked" $La^{(III)}$, $Eu^{(III)}$, and $Yb^{(III)}$ cations were immersed in the [BMI][SCN] or [$MeBu_3N$]-[SCN] liquids, they captured 6 to 8 SCN^- anions, depending on the cation size and on the liquid, without displaying further ligand exchange. Generally, the first 6 SCN^- ligands coordinated early to $Ln^{(III)}$ (during the equilibration stage of the dynamics), while the seventh or eighth ligands complexed up to 2 ns later because of the weaker affinity of the $Ln(NCS)_6^{3-}$ anionic complexes for additional anionic ligands. Finally, $Eu^{(III)}$ became 8-coordinated in [BMI][SCN] and 7-coordinated in [$MeBu_3N$][SCN], while $Yb^{(III)}$ displayed smaller CNs in the two liquids (7 and 6, respectively), as expected from its smaller size. We note that both $Eu^{(III)}$ and $Yb^{(III)}$ ions have higher CNs in the imidazolium than in ammonium-based liquid. The case of $La^{(III)}$ turned out to be somewhat surprising as its final CN was 7 in the two liquids, which is less than for the smaller $Eu^{(III)}$ analogue. This is why we attempted another "dissolution experiment", where $La^{(III)}$ was immersed in [BMI][SCN] in the form of the $La(NCS)_6^{3-}$ complex. In fact, the latter quickly captured two more SCN^- anions, both coordinated via their N atom, to form the $La(NCS)_8^{5-}$ species.

Additional tests (heating-cooling procedure) were performed to confirm the coordination of $La^{(III)}$ and $Yb^{(III)}$ ions in the [BMI][SCN] liquid. For this pupose, we restarted the dynamics of systems that were 7-coordinated and increased the temperature from 300 to 400 K to enhance the diffusion processes. Indeed, the $La(NCS)_7^{4-}$ complex captured an eighth ligand in about 0.8 ns. The latter became first S-coordinated but switched to an N-coordination 0.2 ns later on. On the other hand, the $Yb(NCS)_7^{5-}$ complex did not capture any other ligand, even after 2 ns, supporting its lack of affinity for an additional SCN^- anion.

Average Structural and Solvation Features of the Complexes. The average structural features of $Ln(NCS)_n^{3-n}$ complexes in solution are reported in Table 2. They first show the expected increase in Ln−N distances with the $Ln^{(III)}$ size for a given CN (Ln−N ≈ 2.40, 2.50, and 2.68 Å, respectively, for 8-coordinated $Yb^{(III)}$, $Eu^{(III)}$, and $La^{(III)}$ ions in the [BMI][SCN] IL; Ln−N ≈ 2.34, 2.47, and 2.65 Å, respectively, for the 7-coordinated ions in the [$MeBu_3N$][SCN] IL). Furthermore, for a given $Ln^{(III)}$ ion, Ln−N distances increase with the number of coordinated ligands because of higher ligand−ligand repulsions. For instance, from 7- to 8-coordinated complexes, La−N bonds lengthen by about 0.05 Å, and Eu−N bonds lengthen by about 0.07 Å in the [$MeBu_3N$][SCN] IL. Interestingly, for a given type of complex, Ln−N distances are somewhat longer in the $MeBu_3N^+$ than in the BMI^+-containing liquid (by ca. 0.01 to 0.02 Å for, e.g., $Yb(NCS)_7^{4-}$, $Eu(NCS)_8^{5-}$, or $La(NCS)_8^{5-}$) because of the higher temperature of the former

Table 2. Characterics of the Simulated Solutions and of the Final $Ln(NCS)_n^{3-n}$ Complexes

immersed solute	[cation][SCN]	temperature (K)	time (ns)	final complex	Ln−N(Å)	Ln−N−S(deg)
$La^{(III)}$	197 BMI^+/200 SCN^-	300	5	$La(NCS)_7^{4-}$	2.65	147
$La(NCS)_8^{5-}$	197 BMI^+/192 SCN^-	300	5	$La(NCS)_8^{5-}$	2.68	153
$La^{(III)}$	197 $MeBu_3N^+$/200 SCN^-	400	5	$La(NCS)_7^{4-}$	2.65	155
$La(NCS)_8^{5-}$	197 $MeBu_3N^+$/192 SCN^-	400	5	$La(NCS)_8^{5-}$	2.70	158
$Eu^{(III)}$	197 BMI^+/200 SCN^-	300	5	$Eu(NCS)_8^{5-}$	2.50	157
$Eu(NCS)_8^{5-}$	197 BMI^+/192 SCN^-	300	5	$Eu(NCS)_8^{5-}$	2.51	157
$Eu^{(III)}$	197 $MeBu_3N^+$/200 SCN^-	400	5	$Eu(NCS)_7^{5-}$	2.47	159
$Eu(NCS)_8^{5-}$	197 $MeBu_3N^+$/192 SCN^-	400	5	$Eu(NCS)_8^{5-}$	2.52	161
$Yb^{(III)}$	197 BMI^+/200 SCN^-	300	5	$Yb(NCS)_7^{4-}$	2.33	157
$Yb(NCS)_8^{5-}$	197 BMI^+/192 SCN^-	300	5	$Yb(NCS)_8^{5-}$	2.40	157
$Yb^{(III)}$	197 $MeBu_3N^+$/200 SCN^-	400	5	$Yb(NCS)_6^{3-}$	2.26	157
$Yb(NCS)_8^{5-}$	197 $MeBu_3N^+$/192 SCN^-	400	5	$Yb(NCS)_7^{4-}$	2.34	158
***	135 BMI^+/27 $La(NCS)_8^{5-}$	425	200		2.71[a]	152[a]
***	135 BMI^+/27 $Yb(NCS)_8^{5-}$	425	200		2.34[b]	156[b]

[a] Average taken over the 27 $La(NCS)_8^{5-}$ complexes. [b] Average taken over the 21 $Yb(NCS)_7^{4-}$ complexes.

solutions[55] and the different interactions between the complex and the IL. In solution, the Ln−N−S angles of all complexes are bent, from 147° to 158°, as in the crystal structure of $[BMI]_4[La(NCS)(H_2O)]$ (from 158 to 178°).[16] This contrasts with the gas phase where the NCS^- coordination is linear (see, e.g., the AMBER and QM optimized structures in Supporting Information, Figures S1−S3 and Table S4), suggesting that the bent coordination is due to the interactions of the complex with the surrounding counterions in condensed phases.

In the two studied liquids, anionic $Ln(NCS)_n^{3-n}$ complexes are surrounded by a shell of IL cations, leading to an "onion type solvation" of $Ln^{(III)}$. This can be seen from snaphots (Figure 5) and Ln−N RDFs with either the $N2_{BMI}$ or the N_{MeBu3N} atoms. The IL cation RDFs do not display any marked peak, however. Their integration up to a distance of 10 Å leads to about 14 BMI^+ around $La^{(III)}$ and $Eu^{(III)}$ complexes, and 10 to 13 BMI^+ around $Yb^{(III)}$ complexes in the [BMI][SCN] IL. In the $[MeBu_3N][SCN]$ liquid, one finds less IL cations, about 8 to 11 $MeBu_3N^+$, depending on the system (see Table 3). Thus, the ILs cationic density around the lanthanide complex is smaller in the $MeBu_3N^+$ than in the BMI^+ containing liquid. Furthermore, as described above in the pure liquids, the IL cations display different types of interactions with the complexed SCN^- ligands: BMI^+ cations tend to form H-bonds via their C−H ring protons (see in Figure 6 the proton density peaks around the complexes and the marked peak at about 3 Å in the corresponding RDFs, integrating to 4.2, 4.3, and 4.5 protons, respectively, for the $Yb^{(III)}$, $Eu^{(III)}$, and $La^{(III)}$ complexes), while no specific interactions are observed with $MeBu_3N^+$ cations.

Insights into Energy Features. Results of an energy component analysis, based on the $Ln(NCS)_n^{3-n}$ intracomplex energy ($E_{complex}$) and the interaction energy $E_{complex/IL}$ between the final complex and the remaining ions of the liquid are reported in Table 4. It is quite interesting to first compare different CNs of a given $Ln^{(III)}$. Adding an eighth ligand to a given $Ln(NCS)_7^{4-}$ complex destabilizes the complex itself (by $\Delta E_{Complex} \approx 190$ to 210 kcal/mol, depending on the $Ln^{(III)}$ ion and on the liquid), following trends obtained by Force Field or QM calculations in the gas phase (see Table 1). A similar destabilization is found for the $Yb^{(III)}$ complex when its coordination is increased from 6 to 7 ($\Delta E_{Complex} \approx 150$ kcal/mol in the $[MeBu_3N][SCN]$ liquid). In all cases, however, the $\Delta E_{Complex}$ destabilization is clearly overcome by the gain in "solvation energy" $E_{complex/IL}$ ($\Delta E_{complex/IL} \approx -450$ to -500 kcal/mol in the [BMI][SCN] IL if one compares the 7- to the 8-coordinated $La^{(III)}$ or $Yb^{(III)}$ ions, and about -380 kcal/mol in the $[MeBu_3N][SCN]$ liquid if one compares the 7- to the 8- coordinated $Eu^{(III)}$, as well as the 6- versus 7-coordinated $Yb^{(III)}$ ion). Higher CNs are thus clearly due to enhanced solvation of the more negatively charged complexes.

Comparing now a given $Ln(NCS)_n^{3-n}$ complex in the two types of liquids, one sees that it has very similar internal energies $E_{complex}$ in the two cases, but it is much better solvated in the imidazolium than in the ammonium based liquid: its "solvation energy" $E_{complex/IL}$ is about 100−120 kcal/mol more negative in the former liquid because of the higher cationic charge density around the complex and the stronger (H-bonding) interactions with the SCN^- ligands.

An alternative energy component analysis, focused on the $Ln^{(III)}$ cation as solute, its interaction energy $E_{Ln/IL}$ with all IL ions (involving all SCN^- and BMI^+ or $MeBu_3N^+$ ions), and the internal energy E_{ILIL} of the IL is given in Supporting Information, Table S5. It reveals quite large and antagonistic changes in the $E_{Ln/IL}$ and E_{ILIL} energies as a function of the $Ln^{(III)}$ CN. For instance, from the 7- to the 8-coordinated $La^{(III)}$ ion, $E_{Ln/IL}$ becomes more attractive (by ca. 90 kcal/mol in the [BMI][SCN] liquid and 110 kcal/mol in the $[MeBu_3N][SCN]$ liquid), while the E_{ILIL} energies decrease in magnitude (by ca. 100 and 120 kcal/mol, respectively). Likewise, from the 6- to 7- coordinated $Yb^{(III)}$ ion, $E_{Ln/IL}$ increases by about 120 kcal/mol, while E_{ILIL} decreases by about 100 kcal/mol in the $[MeBu_3N][SCN]$ liquid. Thus, the $Ln^{(III)}$ CN results not only from the metal interactions with the liquid (involving first shell interactions) but also from the internal energy of the liquid itself.[56]

Finally, it would be desirable to compare the total potential energies U_{tot} of systems of identical compositions but with

(55) When the temperature is increased from 300 to 400 K, the average Ln−N distances increase by about 0.01 Å: from 2.68 Å to 2.69 for $La(NCS)_8^{5-}$, from 2.34 Å to 2.35 Å for $Yb(NCS)_7^{4-}$, and from 2.40 Å to 2.41 Å for $Yb(NCS)_8^{5-}$.

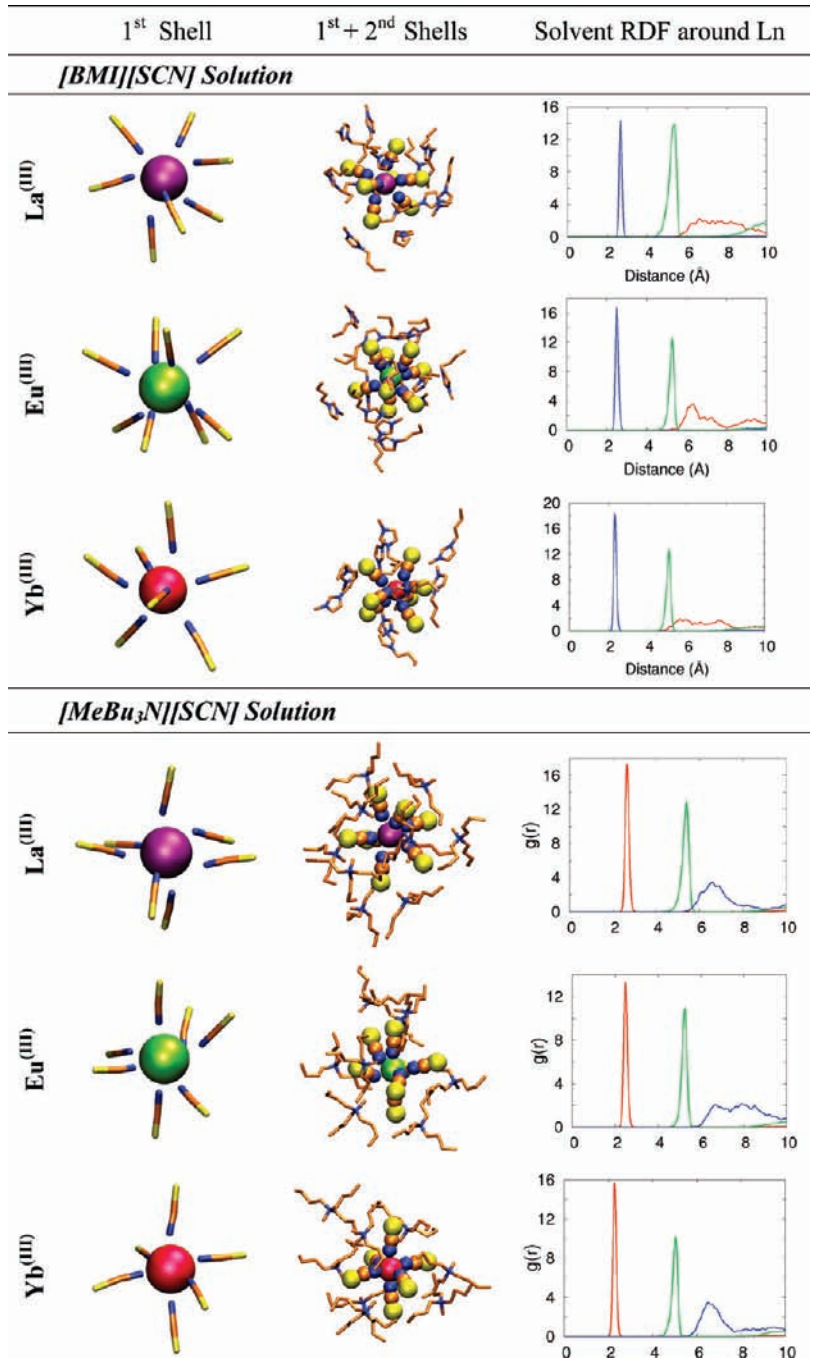

Figure 5. Typical snapshots of the 1st and 2nd solvation shells of the "naked" $Ln^{(III)}$ cation immersed as solute in [BMI][SCN] and [$MeBu_3N$][SCN] solutions. Right: Ln···N_{SCN} (in blue), Ln···S_{SCN} (in green), and Ln···$N2_{BMI}$ (in red) RDFs. A full version, including the results obtained by immersing $Ln(NCS)_8^{5-}$ complexes as solute are given in Supporting Information, Figures S4 and S5.

different CNs of a given $Ln^{(III)}$ ion to gain insighs into their relative stabilities. The differences ΔU_{tot} are generally too small, however, compared to statistical fluctuations (ca. 50 kcal/mol), to safely make conclusions. For instance, in the [BMI][SCN] IL, the ΔU_{tot} difference between 7- and 8-coordinated $La^{(III)}$ containing systems is only 10 kcal/mol. Likewise, for $Yb^{(III)}$, the ΔU_{tot} difference between the 6- and 7- coordinated systems amounts to only 4 kcal/mol in [BMI][SCN]. This is why we have undertaken PMF calcula-

(56) If one compares a given $Ln^{(III)}$ cation in the BMI^+ versus $MeBu_3N^+$ containing liquids, it is found to have a more negative $E_{Ln/IL}$ interaction energy with the latter. This is due to the IL cations repulsions with $Ln^{(III)}$ which are higher with BMI^+ than with $MeBu_3N^+$.

(57) Arguably, the [BMI][SCN] and [$MeBu_3N$][SCN] solutions have been simulated at different temperatures, 300 K and 400K, respectively. This temperature effect is small however, as seen for the $La(NCS)_8^{5-}$ and $Yb(NCS)_8^{5-}$ complexes that display similar interaction energies $E_{complex/IL}$ with the [BMI]SCN] liquid at both temperatures (see Table 4). The differences $\Delta E_{complex/IL}$ amount to 15 and 2 kcal/mol, respectively, for these complexes. This is small, compared to energy differences observed from one liquid to the other. See also the recent theoretical study on the La^{3+} hydration in the 277−623 K temperature range, showing that "temperature has virtually no effect on the first hydration shell structural properties"Duvail, M.; Spezia, R.; Cartailler, T.; Vitorge, P. *Chem. Phys. Lett.* **2007**, *448*, 41–45.

Table 3. Characteristics of the First Peak of the [BMI][SCN] and [$MeBu_3N$][SCN] RDFs around the $Ln^{(III)}$ Cation in Solution[a]

immersed solute	final complex	Ln−N_{SCN}	Ln−S_{SCN}	Ln−N[b]
[BMI][SCN] Solution				
$La^{(III)}$	$La(NCS)_7^{4-}$	7 (2.6; 3.1)	7 (5.3; 5.8)	14.5[c]
$La(NCS)_7^{4-}$ *(400 K)*	$La(NCS)_8^{5-}$	8 (2.7; 3.1)	8 (5.4; 5.8)	15.2[c]
$La(NCS)_8^{5-}$	$La(NCS)_8^{5-}$	8 (2.7; 3.0)	8 (5.4; 5.8)	14.1[c]
$Eu^{(III)}$	$Eu(NCS)_8^{5-}$	8 (2.5; 2.9)	8 (5.3; 5.6)	13.7[c]
$Eu(NCS)_8^{5-}$	$Eu(NCS)_8^{5-}$	8 (2.5; 2.9)	8 (5.3; 5.7)	15.6[c]
$Yb^{(III)}$	$Yb(NCS)_7^{4-}$	7 (2.3; 2.7)	7 (5.1; 5.4)	10.5[c]
$Yb(NCS)_8^{5-}$	$Yb(NCS)_8^{5-}$	8 (2.4; 2.8)	8 (5.2; 5.6)	13.3[c]
$Yb(NCS)_8^{5-}$ *(400 K)*	$Yb(NCS)_8^{5-}$	8 (2.4; 3.0)	8 (5.1; 5.9)	13.5[c]
[$MeBu_3N$][SCN] Solution				
$La^{(III)}$	$La(NCS)_7^{4-}$	7 (2.6; 3.0)	7 (5.4; 5.8)	7.7[c]
$La(NCS)_8^{5-}$	$La(NCS)_8^{5-}$	8 (2.7; 3.1)	8 (5.5; 5.9)	9.5[c]
$Eu^{(III)}$	$Eu(NCS)_7^{4-}$	7 (2.5; 2.8)	7 (5.2; 5.6)	9.6[c]
$Eu(NCS)_8^{5-}$	$Eu(NCS)_8^{5-}$	8 (2,5; 3.0)	8 (5.3; 5.9)	9.7[c]
$Yb^{(III)}$	$Yb(NCS)_6^{3-}$	6 (2.3; 2.5)	6 (5.0; 5.4)	7.9[c]
$Yb(NCS)_8^{5-}$	$Yb(NCS)_7^{4-}$	7 (2.4; 2.7)	7 (5.1; 5.5)	11.0[c]

[a] Integration number of the first peak whose maximum and minimum are given in parenthesis (in Å). [b] N is either the $N2_{BMI}$ atom of BMI^+ or the N atom of $MeBu_3N^+$. [c] No clearly defined 1st peak, integration up to 10 Å.

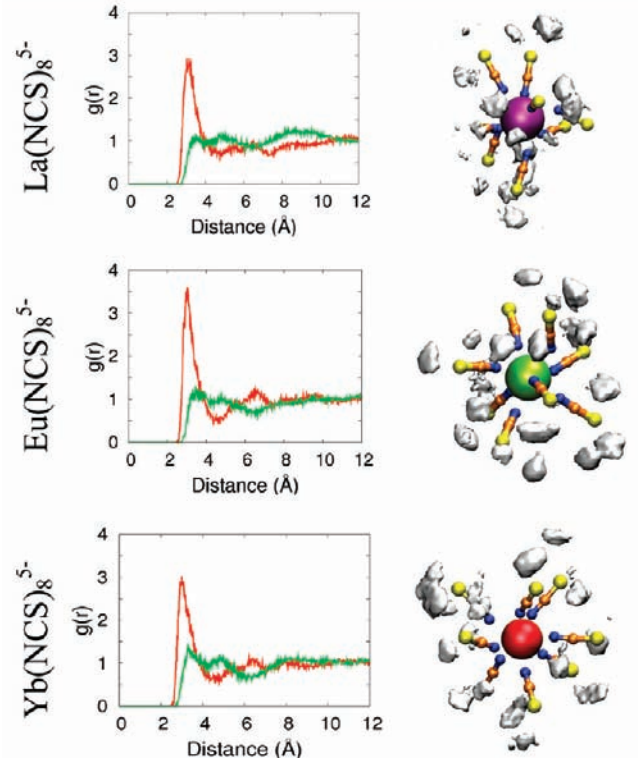

Figure 6. Solvation of SCN^- ligands of the $Ln(NCS)_n^{3-n}$ complexes by imidazolium protons. Left: radial distribution functions of the imidazolium ring protons (red) and the CH_3(butyl) protons (green) around the S atoms. Right: density maps of imidazolium ring protons around the NCS^- anions (accumulated during the last nanosecond).

tions on the addition of a SCN^- anion to selected complexes in solution (see next section).

4. PMF Calculations on 7- versus 8-Coordination of SCN^- to $La^{(III)}$, $Eu^{(III)}$, and $Yb^{(III)}$ in the [BMI][SCN] and [$MeBu_3N$][SCN] ILs. We have seen several cases where MD simulations starting from different configurations lead to different CNs in a given liquid. To more precisely assess the free energy difference between 7- and 8-coordinations, we decided to calculate the free energy profiles (potential

Table 4. Energy Component Analysis (kcal/mol), Based on the Final $Ln(NCS)_n^{3-n}$ Complex, and Its Interaction with the Remaining IL Ions[a]

immersed solute	final complex	$E_{complex}$	$E_{complex/IL}$	E_{ILIL}	U_{tot}
[BMI][SCN] Solution					
$La^{(III)}$	$La(NCS)_7^{4-}$	−353 (5)	−993 (18)	−446	−1792 (40)
$La(NCS)_7^{4-}$ *(400 K)*	$La(NCS)_8^{5-}$	−141 (8)	−1480 (28)	1431	−190 (56)
$La(NCS)_8^{5-}$	$La(NCS)_8^{5-}$	−167 (41)	−1465 (21)	−157	−1789 (38)
$Eu^{(III)}$	$Eu(NCS)_8^{5-}$	−206 (4)	−1485 (19)	−147	−1838 (40)
$Eu(NCS)_8^{5-}$	$Eu(NCS)_8^{5-}$	−225 (42)	−1483 (18)	−168	−1876 (39)
$Yb^{(III)}$	$Yb(NCS)_7^{4-}$	−479 (4)	−995 (17)	−420	−1894 (39)
$Yb(NCS)_8^{5-}$	$Yb(NCS)_8^{5-}$	−269 (40)	−1494 (20)	−146	−1909 (40)
$Yb(NCS)_8^{5-}$ *(400 K)*	$Yb(NCS)_8^{5-}$	−259 (33)	−1493 (26)	1443	−309 (54)
[$MeBu_3N$][SCN] Solution					
$La^{(III)}$	$La(NCS)_7^{4-}$	−362 (5)	−910 (18)	305	−937 (66)
$La(NCS)_8^{5-}$	$La(NCS)_8^{5-}$	−170 (31)	−1362 (20)	593	−939 (67)
$Eu^{(III)}$	$Eu(NCS)_7^{4-}$	−429 (5)	−908 (17)	331	−1006 (67)
$Eu(NCS)_8^{5-}$	$Eu(NCS)_8^{5-}$	−226 (32)	−1380 (21)	622	−984 (70)
$Yb^{(III)}$	$Yb(NCS)_6^{3-}$	−647 (4)	−555 (14)	212	−990 (69)
$Yb(NCS)_8^{5-}$	$Yb(NCS)_7^{4-}$	−493 (25)	−937 (18)	423	−1007 (64)

[a] Averages and fluctuations (in parentheses) over the last nanosecond.

of mean force "PMF" calculations) for complexation of an eighth SCN^- anion by $Ln(NCS)_7^{4-}$ complexes (Ln = La, Eu and Yb) in [BMI][SCN] and [$MeBu_3N$][SCN] solutions. We also studied the SCN^- complexation by $Yb(NCS)_6^{3-}$ in [$MeBu_3N$][SCN] to compare the 6- to 7- coordinations. The PMF simulations started with the uncoordinated SCN^- anion that sits at the shortest distance from $Ln^{(III)}$ at the end of the dynamics (Ln−N ≈ 8.5 Å, that is, beyond the first cationic shell) and was then stepwise coordinated to $Ln^{(III)}$.

Free energy profiles calculated for the different $Ln^{(III)}$ cations, using different equilibration and sampling times, are reported in Figure 7. In the $La^{(III)}$ case, the free energy profiles show that complexation of an eighth SCN^- ligand by the 7-coordinated cation is favored, by −7 to −15 kcal/mol in [BMI][SCN] and by −4 to −5 kcal/mol in [$MeBu_3N$][SCN]. The free energy difference between the 7- and 8-coordinated complexes is thus less pronounced in [$MeBu_3N$][SCN] than in [BMI][SCN]. This is consistent with the fact that $La(NCS)_8^{5-}$ is more stabilized than $La(NCS)_7^{4-}$ by the [BMI][SCN] liquid compared to the [$MeBu_3N$][SCN] liquid (the differences amount to about 100 and 80 kcal/mol, respectively; see Table 4).[57]

Free energy profiles for the coordination of an eigth SCN^- ligand to $Eu(NCS)_7^{4-}$ show that this reaction is slightly favored (by about −2 kcal/mol) in [BMI][SCN] but is clearly endergonic (by +8 to +12 kcal/mol) in [$MeBu_3N$][SCN], in keeping with a higher stabilization of the $Eu(NCS)_8^{5-}$ complex by BMI^+ compared to $MeBu_3N^+$ cations.

In the case of the small cation $Yb^{(III)}$, the three free energy profiles in [BMI][SCN] indicate that the approach of an eighth ligand is unfavored (by 2 to 5 kcal/mol), likely because of increased repulsions between the SCN^- ligands that are more tightly coordinated than in the $Eu^{(III)}$ or $La^{(III)}$ complexes. In [$MeBu_3N$][SCN] the coordination of the eighth ligand is also endergonic, but by a higher amount (8 to 15 kcal/mol). These PMF results are consistent with the observed loss of a SCN^- ligand from $Yb(NCS)_8^{5-}$ during the free dynamics in the [$MeBu_3N$][SCN] liquid but not in the [BMI][SCN] liquid (vide supra). On the other hand, the

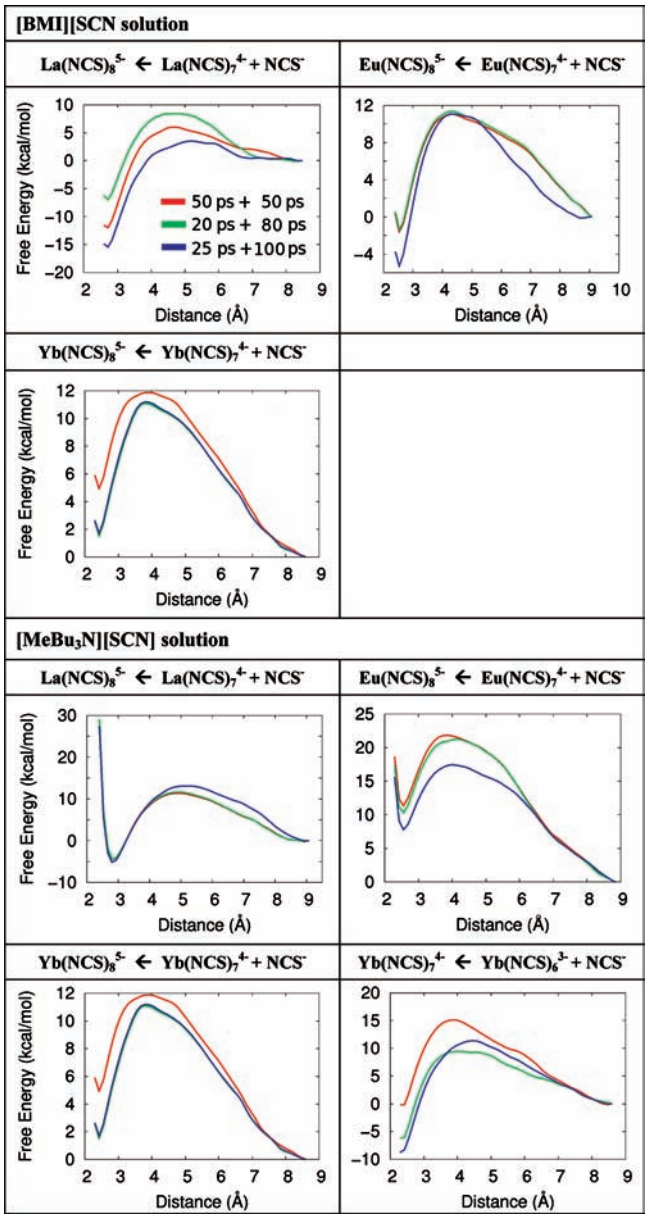

Figure 7. Calculated free energy profiles for the complexation of an additional NCS^- ligand by the $Ln(NCS)_7^{4-}$ complexes in the two ILs, and by the $Yb(NCS)_6^{3-}$ complex in the $[MeBu_3N][SCN]$ liquid. Calculations with different equilibration and sampling times at each window: 50 + 50 ps (red curve), 20 + 80 ps (green curve), or 25 + 100 ps (blue curve). See text.

free energy profiles for SCN^- complexation by $Yb(NCS)_6^{3-}$ in $[MeBu_3N][SCN]$ show that this process is favored (by −1 to −9 kcal/mol, depending on the simulation protocol), confirming that $Yb^{(III)}$ is hepta-coordinated.

5. $[BMI]_5[Ln(NCS)_8]$ IL. In this section, we report MD simulation results on two $[BMI]_5[Ln(NCS)_8]$ liquids, formally based on BMI^+ cations and $Ln(NCS)_8^{5-}$ anions, with Ln = La and Yb, respectively. The simulations were started from a 3 × 3 × 3 grid of preformed $Ln(NCS)_8^{5-}$ complexes surrounded by BMI^+ cations. After 200 ns of dynamics of the $[BMI]_5[La(NCS)_8]$ liquid with the bigger lanthanide cation, all 27 complexes cations retained an 8-coordination, as did the $La(NCS)_8^{5-}$ complex in the [BMI][SCN] solution. On the average, each $La(NCS)_8^{5-}$ complex was surrounded by 10 BMI^+ cations within 9 Å, and the shortest La−La distance was 12.8 Å.

To test the possible impact of the starting configuration on the lanthanide CN, we decided to mix the $[BMI]_5[La(NCS)_8]$ liquid to generate a random distribution of BMI^+ and SCN^- ions. Mixing was achieved by a MD simulation of 2 ns at a temperature of 500 K, with Coulombic interactions scaled down by a factor 100 to enhance the sampling, while freezing the $La^{(III)}$ ions at their initial positions to maintain a reasonable distribution. This was followed by a "demixing" simulation of 200 ns at a temperature of 425 K and at constant volume. During this MD simulation, the number of N-coordinated ligands increased regularly. Indeed, at the beginning (0 ns), there were only 8 $La(NCS)_8^{5-}$ complexes, and different mixed complexes with S- and N-coordinated ligands, sometimes with lower CNs. After 200 ns one finds about 15 $La(NCS)_8^{5-}$ complexes with all N-coordinated ligands and 12 $La(NCS)_7(SCN)_1^{5-}$ complexes where one ligand, on the average, is S-coordinated. Visual inspection of the trajectories and La···La RDFs (see Supporting Information, Figure S6) indicates that the S-coordinated ligands are in fact N-coordinated to another $La^{(III)}$ ion and involved in La···SCN···La bridging interactions (see Figure 8). One thus finds $La^{(III)}$ complexes forming dimers (3) and trimers (2) sharing a SCN^- bridging ligand, leading to shorter La···La distances (7.2 to 8.4 Å) than in the IL containing only $La(NCS)_8^{3-}$ monomeric complexes (12.8 Å). During the 200 ns dynamics, some dimers evolved toward $La(NCS)_8^{5-}$ monomers with eight N-coordinated ligands which, according to the QM and force field calculations reported above, are preferred over S-coordinated ligands. Furthermore, comparison of the total energies of this mixed-demixed liquid and of the "original liquid" with octa-coordinated $La(NCS)_8^{5-}$ complexes shows that the latter is more stable (by ca. 120 ± 50 kcal/mol during the last ns) and should thus be preferred.

The $[BMI]_5[Yb(NCS)_8]$ liquid based on the smaller $Yb^{(III)}$ cation was also simulated for 200 ns, starting with 27 prebuilt $Yb(NCS)_8^{5-}$ complexes. In that case, only six complexes remained 8-coordinated while the majority (21 complexes) lost one SCN^- ligand to form the $Yb(NCS)_7^{4-}$ species. This is consistent with the stoichiometry observed above in the [BMI][SCN] liquid.

The dynamics of these liquids displays an interesting feature, as their BMI^+ cations diffuse much more rapidly than their anionic complexes. This can be seen from cumulated views of selected ions (Figure 9) and is further supported by calculated diffusion coefficients, D, that are about about 10 times larger for BMI^+ than for $Ln^{(III)}$ cations (in 10^{-8} cm^2/s): 4.0 versus 0.3 in $[BMI]_5[La(NCS)_8]$ and 2.6 versus 0.2 in $[BMI]_5[Yb(NCS)_8]$. The BMI^+ ions diffusion is thus slower in the $Yb^{(III)}$ than in the $La^{(III)}$ containing liquids and slower than in the pure [BMI][SCN] liquid. The structure of the two studied liquids of $[BMI]_5[Ln(NCS)_8]$ composition

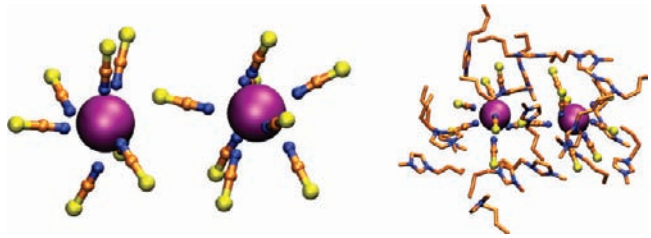

Figure 8. La···La dimer with a SCN^- bridging ligand formed during the 200 ns MD simulation of the "randomly mixed" $[BMI]_5[La(NCS)_8]$ IL.

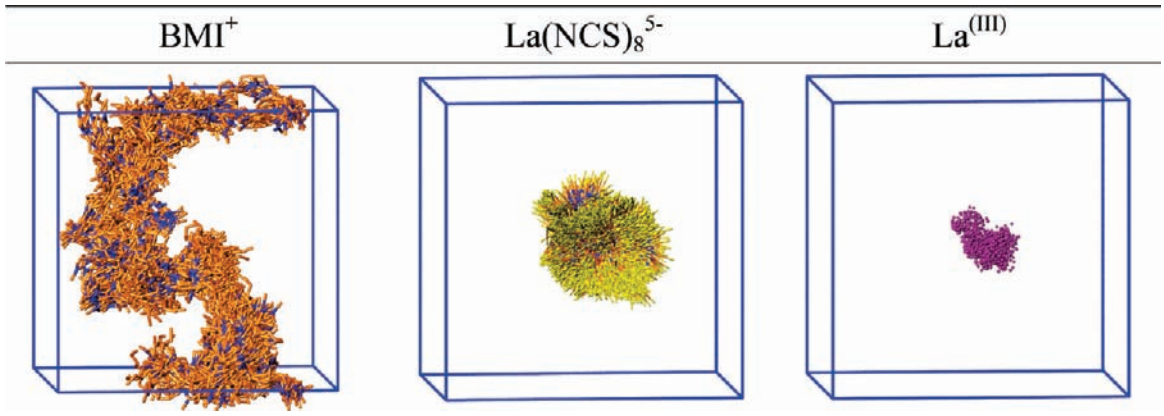

Figure 9. Pure $[BMI]_5[La(NCS)_8]$ liquid: Cumulated views over 200 ns of one BMI^+ (left), one $La(NCS)_8^{5-}$ complex (middle), and one $La^{(III)}$ cation (right).

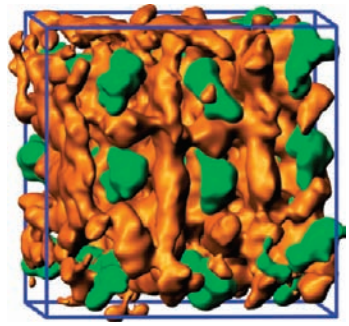

Figure 10. Pure $[BMI]_5[La(NCS)_8]$ IL: Highest density regions of $La^{(III)}$ cations (green) and of BMI^+ cations (orange).

can thus be seen as a more or less frozen network formed of $Ln(NCS)_8^{5-}$ or $Ln(NCS)_7^{4-}$ complexes surrounded by a viscous fluid made of BMI^+ cations (Figure 10).

Discussion

We report a MD study of the pure [BMI][SCN] and $[MeBu_3N][SCN]$ ILs with the main aim to investigate their solvation properties toward $Ln^{(III)}$ lanthanide cations. This is a quite challenging task because of the soft (polarizable) and ambidentate nature of the constitutive SCN^- anions. In fact, the parameters we developed, based on an empirical 1-6-12 representation of the interactions between ionic species, satisfactorily account for the interaction energy between BMI^+ and SCN^- (this is crucial to model the liquid itself), for the energy difference between N- versus S-coordination of SCN^- in hexa-coordinated complexes and for the spontaneous N-coordination of solvent anions to $Ln^{(III)}$ and $Ln(NCS)_6^{3-}$ species immersed in the ILs. They also account for the energy evolution of successive coordination of up to 8 SCN^- anions to $Ln^{(III)}$ cations, as compared to the QM (HF or DFT) results. This does not mean that electronic reorganization effects (mainly anion to cation charge transfer and anion polarization) are negligible.[18,58,59] See for instance the Mulliken atomic charges obtained from DFT and HF optimizations (Supporting Information, Table S6), indicating reduced charge magnitude on $Ln^{(III)}$ and N atoms as the number of SCN^- ligands increases. Likewise, for a given CN, q(Ln) charges decrease in the order $La^{(III)} > Eu^{(III)} > Yb^{(III)}$, reflecting stronger interactions when the cation gets smaller. Such electronic effects should be included in more refined force field treatments, as achieved, for example, in water.[60] In a more remote perspective, MD based on QM calculated energies and forces should be developed (see, e.g., refs 61, 62 for CP-MD studies of Gd^{3+} complexes in water, and refs 63−66 for ILs). However, as mentioned in the introduction, the sampling of the most important configurations and, particularly, the CNs of $Ln^{(III)}$ ions represents a major issue and requires long simulations. The lack of full convergence, depending on the initial state, observed for

(58) Yan, T.; Burnham, C. J.; Del Popolo, M. G.; Voth, G. A. *J. Phys. Chem. B* **2004**, *108*, 11877–11881.
(59) Borodin, O.; Smith, G. D. *J. Phys. Chem. B* **2006**, *110*, 6293–6299.
(60) Kowall, T.; Foglia, F.; Helm, L.; Merbach, A. E. *J. Am. Chem. Soc.* **1995**, *117*, 3790–3799.
(61) Pollet, R.; Marx, D. *J. Chem. Phys.* **2007**, *126*, 181102.
(62) Yazyev, O. V.; Helm, L. *J. Chem. Phys.* **2007**, *127*, 084506.
(63) Del Popolo, M. G.; Lynden-Bell, R. M.; Kohanoff, J. *J. Phys. Chem. B* **2005**, *109*, 5895–5902.
(64) Bühl, M.; Chaumont, A.; Schurhammer, R.; Wipff, G. *J. Phys. Chem. B* **2005**, *109*, 18591–18599.
(65) Kirchner, B.; Seitsonen, A. P.; Hutter, J. *J. Phys. Chem. B* **2006**, *110*, 11475–11480.
(66) Bhargava, B. L.; Balasubramanian, S. *Chem. Phys. Lett.* **2006**, *417*, 486–491.

$La^{(III)}$ and $Yb^{(III)}$ solutes, points to the need of at least multi-nanosecond simulation times, presently precluding sophisticated representations of the potential energy. As found previously for the simulated $EuCl_n^{3-n}$ and EuF_n^{3-n} complexes,[26] 1-6-12 AMBER results account for the main structural and energy features of the $Ln(NCS)_n^{3-n}$ complexes (compare for instance AMBER versus QM calculated lenghtening of Ln−N bonds when the $Ln^{(III)}$ cation gets bigger or when the CN increases; Supporting Information, Table S7). We thus feel that there is no major artifact in the simulated results.

Regarding the number of SCN^- ligands coordinated to $Ln^{(III)}$ in solution (7 to 8, depending on the cation), it is first worth looking at QM (HF and DFT) and AMBER results on the successive addition of ligands (Table 2). In fact, both types of methods indicate that, for the three studied $Ln^{(III)}$ cations, hexa-complexes $Ln(NCS)_6^{3-}$ are intrinsically unstable and should loose one to two ligands in the gas phase. Indeed, once an anionic complex is formed (e.g., $Ln(NCS)_5^{2-}$), its affinity for additional ligands is too small to overcome the increased ligand−ligand repulsions. This contrasts with the IL solution where, in spite of their −3 charge, the three studied $Ln(NCS)_6^{3-}$ complexes capture one to two more SCN^- ligands because of solvation effects. Indeed, these anionic complexes are solvated by a first shell of BMI^+ or $MeBu_3N^+$ cations, following the "onion type" alternation of ionic shells around $Ln^{(III)}$, as reported for $EuCl_6^{3-}$, EuF_6^{3-}, and UCl_6^{3-} anionic complexes in ILs.[26,27,33] In solid state structures, the $Ln(NCS)_n^{3-n}$ anionic complexes are likewise surrounded by organic (quaternary ammonium) counterions (see Supporting Information, Table S1 and ref 30 for a review of X-ray structures). The latter stabilize the anionic complex via Coulombic interactions and, in the case of the imidazolium based liquids, via hydrogen bonding interactions between their C−H aromatic protons and S_{SCN} atoms. Similar H-bonds with SCN^- ligands have been observed in solid state structures of $Ln(NCS)_x(H_2O)_y^{3-x}$.[16] There are also analogues with halide complexes of LnX_6^{3-}, $UO_2X_4^{2-}$, or UX_6^{2-} type in the solid state [67,68] or in solution.[69]

Interestingly, according to our simulations, a given $Ln^{(III)}$ cation tends to have a higher CN in the [BMI][SCN] than in the $[MeBu_3N][SCN]$ liquid. For instance, free energy calculations indicate that the big $La^{(III)}$ ion prefers 8- over 7-coordination in both liquids, but the energy difference between both types of complexes is highest in the imidazolium containing liquid. Conversely, the small $Yb^{(III)}$ cation prefers the 7- over the 8-coordination in both liquids but by a larger amount in the ammonium than in the imidazolium based liquid. The $Eu^{(III)}$ case is intermediate, since it clearly prefers the 7-coordination in the ammonium containing liquid, while it slightly prefers the 8-coordination in the imidazolium based IL. High CNs correspond to highly charged anionic complexes that are stabilized by a high density of surrounding positive charges and by specific H-bonding interactions and are thus favored by BMI^+ rather than by NR_4^+ counterions. These findings are consistent with the observed stoichiometries of $Ln^{(III)}$ complexes with SCN^- ligands and NR_4^+ counterions bearing different alkyl chains: in solid state structures, high/small numbers of SCN^- anions correspond to small/big NR_4^+ ions (see Supporting Information, Table S1). For instance, when the counterion is changed from Et_4N^+ to Me_4N^+, $Yb^{(III)}$ moves from a 6- to a 7-coordination; likewise, while $Eu^{(III)}$ is 8-coordinated with Me_4^+ as counterion, its $Er^{(III)}$ analogue of similar size is only 6-coordinated with NBu_4^+ as counterion.[70] Thus, the precise nature of the counterion markedly influences the stoichiometry of the complex and thereby the nature of the $[cation]_m[Ln(NCS)_n]$ IL based on it. Similar effects are expected to operate in liquid−crystalline phases involving, for example, imidazolium cations with extended alkyl chains.[15]

The simulated solutions can be viewed as resulting, for example, from the dissolution of a $Ln(SCN)_6^{3-}$ 3 BMI^+ salt in the [BMI][SCN] or $[MeBu_3N][SCN]$ liquids, showing that the $Ln^{(III)}$ CN should increase to 7 or 8. This contrasts with the case of halides that remain hexacoordinated to $Ln^{(III)}$ in ILs.[15,67,71−74] Note that our systems are dry, and that water, even present in small amounts, would compete with SCN^- to coordinate $Ln^{(III)}$. To our knowledge, this has not been studied with SCN^- ligands but is well documented from spectroscopic[15] and simulation[23] studies with other anions. Water also influences the physical state of lanthanide salts. For instance, $Ln(NCS)_3(H_2O)_n$ hydrated complexes ($n = 5$ to 7, depending on the size of $Ln^{(III)}$) crystallize in conditions where dry $Ln(NCS)_3$ does not form crystals.[30] Regarding ILs based on $Ln(NCS)_n^{3-n}$ anionic complexes, they crystallize with one co-complexed H_2O molecule but not in dry conditions.[16] Thus, the CN of the $Ln^{(III)}$ lanthanide by SCN^- ligands in IL solution depends not only on the nature of the counterion but also on the purity of the IL (humidity, traces of other competing anions like halides), as well as on the nature of the dissolved salt.[22−29] Our results should stimulate experiments along these lines, and on the computational side, simulations on ILs based on anionic lanthanide complexes like $Ln(NCS)_n^{3-n}$ 3 M^+, as a function of the $Ln^{(III)}$, of the IL M^+ cationic species, and of added "impurities".

(67) Pellens, M.; Thijs, B.; van Hecke, K.; van Meervelt, L.; Binnemans, K.; Nockemann, P. *Acta Crystallogr., Section E* **2008**, *E64*, m945.
(68) Deetlefs, M.; Hitchcock, P. B.; Hussey, C. L.; Mohammed, T. J.; Seddon, K. R.; Van der Berg, J. A.; Zora, J. A. In *Ionic liquids IIIA: fundamentals, progress, challenges and opportunities. Properties and structure*; Rogers, R. D., Seddon, K. R., Eds.; American Chemical Society: Washington, DC, 2005; Chapter 4, pp 47−67.
(69) Bossé, E.; Den Auwer, C.; Berthon, C.; Guilbaud, P.; Grigoriev, M. S.; Nikitenko, S.; Naour, C. L.; Cannes, C.; Moisy, P. *Inorg. Chem.* **2008**, *47*, 5746–5755.
(70) Burmeister, J. L.; Patterson, S. D.; Deardorff, E. *Inorg. Chim. Acta* **1969**, *3*, 105–109.
(71) Matsumoto, K.; Tsuda, T.; Nohira, T.; Hagiwara, R.; Ito, Y.; Tamada, O. *Acta Crystallogr., Sect. C: Cryst. Struct. Commun.* **2002**, *C58*, m186–m187.
(72) Photiadis, G. M.; Borresen, B.; Papatheodorou, G. N. *J. Chem. Soc., Faraday Trans.* **1998**, *94*, 2605–2613.
(73) Lipsztajn, M.; Osteryoung, R. A. *Inorg. Chem.* **1985**, *24*, 716–719.
(74) Gau, W. J.; Sun, I. W. *J. Electrochem. Soc.* **1996**, *143*, 914–919.

Acknowledgment. The authors are grateful to IDRIS, CINES, Université Louis Pasteur, and GDR CNRS PARIS for computer resources, and to Etienne Engler for assistance. G.W. is grateful to late Mimine for 20 years of sympathetic ear and support.

Supporting Information Available: Further details are given in Tables S1−S7 and Figures S1−S6. This material is available free of charge via the Internet at http://pubs.acs.org.

IC802227P